



# Predicting cyanobacteria bloom occurrence in lakes and reservoirs before blooms occur

C.S. Zhao <sup>a,f</sup>, N.F. Shao <sup>b</sup>, S.T. Yang <sup>a,g,\*</sup>, H. Ren <sup>e</sup>, Y.R. Ge <sup>c</sup>, P. Feng <sup>c</sup>, B.E. Dong <sup>d</sup>, Y. Zhao <sup>c</sup>

<sup>a</sup> College of Water Sciences, Beijing Normal University, Beijing Key Laboratory of Urban Hydrological Cycle and Sponge City Technology, Beijing 100875, PR China

<sup>b</sup> School of Geography, Faculty of Geographical Science, Beijing Normal University, Beijing 100875, PR China

<sup>c</sup> Jinan Survey Bureau of Hydrology and Water Resources, Jinan 250013, PR China

<sup>d</sup> Dongying Bureau of Hydrology and Water Resources, Dongying 257000, PR China

<sup>e</sup> Administration of Yanma Reservoir, Zaozhuang 277200, PR China

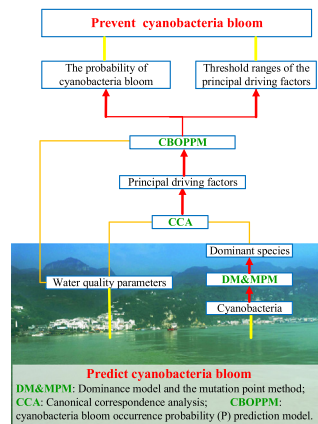
<sup>f</sup> ICube, Uds, CNRS (UMR 7357), 300 Bld Sebastien Brant, CS 10413, 67412 Illkirch, France

<sup>g</sup> Guizhou Normal University, Guiyang 550001, PR China

## HIGHLIGHTS

- Our method can analyze probability and driving factors before cyanobacteria bloom occur.
- Studies from other regions approved our method and results.
- Probability of 0.75 is a critical point for cyanobacteria bloom prevention.
- It can effectively predict cyanobacteria blooms and help reduce occurrence risk.

## GRAPHICAL ABSTRACT



## ARTICLE INFO

### Article history:

Received 28 November 2018  
 Received in revised form 28 February 2019  
 Accepted 11 March 2019  
 Available online 12 March 2019

Editor: Frederic Coulon

### Keywords:

Water quality  
 Cyanobacterial blooms  
 Canonical correspondence analysis

## ABSTRACT

With increased global warming, cyanobacteria are blooming more frequently in lakes and reservoirs, severely damaging the health and stability of aquatic ecosystems and threatening drinking water safety and human health. There is an urgent demand for the effective prediction and prevention of cyanobacterial blooms. However, it is difficult to effectively reduce the risks and loss caused by cyanobacterial blooms because most methods are unable to successfully predict cyanobacteria blooms. Therefore, in this study, we proposed a new cyanobacterial bloom occurrence prediction method to analyze the probability and driving factors of the blooms for effective prevention and control. Dominant cyanobacterial species with bloom capabilities were initially determined using a dominant species identification model, and the principal driving factors of the dominant species were then analyzed using canonical correspondence analysis (CCA). Cyanobacterial bloom probability was calculated using a newly-developed model, after which, the probable mutation points were identified and thresholds for the principal driving factors of cyanobacterial blooms were predicted. A total of 141 phytoplankton data sets from 90 stations were collected from six large-scale hydrology, water-quality ecology, integrated field surveys in Jinan

\* Corresponding author.  
 E-mail addresses: [13838364631@163.com](mailto:13838364631@163.com) (N.F. Shao), [pacorrespondence@126.com](mailto:pacorrespondence@126.com) (S.T. Yang).

City, China in 2014–2015 and used for model application and verification. The results showed that there were six dominant cyanobacterial species in the study area, and that the principal driving factors were water temperature, pH, total phosphorus, ammonia nitrogen, chemical oxygen demand, and dissolved oxygen. The cyanobacterial blooms corresponded to a threshold water temperature range, pH, total phosphorus (TP), ammonium nitrogen level, chemical oxygen demand, and dissolved oxygen levels of 19.5–32.5 °C, 7.0–9.38, 0.13–0.22 mg L<sup>-1</sup>, 0.38–0.63 mg L<sup>-1</sup>, 10.5–17.5 mg L<sup>-1</sup>, and 4.97–8.28 mg L<sup>-1</sup>, respectively. Comparison with research results from other global regions further supported the use of these thresholds, indicating that this method could be used in habitats beyond China. We found that the probability of cyanobacterial bloom was 0.75, a critical point for prevention and control. When this critical point was exceeded, cyanobacteria could proliferate rapidly, increasing the risk of cyanobacterial blooms. Changes in driving factors need to be rapidly controlled, based on these thresholds, to prevent cyanobacterial blooms. Temporal and spatial scales were critical factors potentially affecting the selection of driving factors. This method is versatile and can help determine the risk of cyanobacterial blooms and the thresholds of the principal driving factors. It can effectively predict and help prevent cyanobacterial blooms to reduce the global probability of occurrence, protect the health and stability of water ecosystems, ensure drinking water safety, and protect human health.

© 2019 Elsevier B.V. All rights reserved.

## 1. Introduction

With the development of industry and agriculture, large amounts of nutrients discharged into rivers and lakes, and the eutrophication of water bodies has continued to increase (Eom et al., 2017; Cremona et al., 2018; Zhao et al., 2018). The increase in global warming is causing frequent water bloom (Joehnk et al., 2008). The massive propagation and decay of algae reduces the dissolved oxygen content of the water, leading to the death of aquatic animals and severely damaging aquatic ecosystems (O'Boyle et al., 2016). Cyanobacterial blooms also produce a variety of biological toxins, the most common and harmful being microcystin (Scherer et al., 2017; Dalu and Wasserman, 2018), which can damage tissues such as the liver, kidney, heart, gonads, and nervous system of vertebrates (Yang et al., 2016; Zi et al., 2018). Outbreaks of cyanobacteria not only jeopardize the health of aquatic ecosystems, but also severely affect drinking water safety, and consequently human health (Brookes and Carey, 2011; Carmichael and Boyer, 2016; Tollefson, 2018).

Cyanobacteria have unique physiological characteristics, making it easy for them to become dominant species and form blooms (Su et al., 2019). First, they are among the simplest unicellular prokaryotes; the cells have pseudo vacuoles or pseudo vacuole clusters, and adjusting their buoyancy allows them to occupy a favorable light energy absorption position in the water column (Reynolds et al., 1981). Second, most cyanobacteria have a glial cell coating composed of microfibrils, which serve important functions, such as protection against herbivorous grazing and digestion (Hu, 2011). Third, cyanobacteria utilize exopolysaccharides to aggregate single cyanobacteria cells into groups and form air-filled intercellular spaces to create buoyancy, physically facilitating the formation of cyanobacterial blooms (Zhang et al., 2011; Xiao et al., 2012). Lastly, cyanobacteria can efficiently absorb and concentrate low concentrations of CO<sub>2</sub> (Espie et al., 1988) and easily store excess nutrients (Pettersson et al., 1993). Nitrogen-fixing cyanobacteria can also convert and absorb nitrogen from the air (Blomqvist et al., 1994), rendering cyanobacteria more competitive than other algae.

The occurrence of cyanobacterial blooms is usually affected by environmental conditions, especially water quality (Park et al., 2017; Bucak et al., 2018) (Table 1). Algal proliferation depends on nutrient availability. Slow flow rates in lakes and reservoirs and insufficient water self-purification capacities, with a long renewal period, can lead to nutrient accumulation, and consequently, conditions conducive to cyanobacterial blooms (Havens et al., 2001; Arhonditsis and Brett, 2005; Wang et al., 2016; Kozak et al., 2019). Under sufficient nutrient conditions, cyanobacterial blooms are also affected by various factors, such as water temperature (Descy et al., 2016), pH (Teixeira de Oliveira et al., 2011), and light (Soares et al., 2009) (Table 1). It is important to identify dominant cyanobacterial species and major water quality factors that drive cyanobacterial blooms, as well as determine the

threshold ranges of principal driving factors, to prevent and control cyanobacterial blooms (Huber et al., 2012).

Recent studies on the principal driving factors behind cyanobacterial blooms (Table 1) are based predominantly on all cyanobacterial data in the study area without identifying prior and crucial species (Phlips et al., 2011; Duan et al., 2018). Furthermore, the analysis of cyanobacteria is often based on data at the genus level (Tian et al., 2013; Hu et al., 2018); therefore, interspecies differences within a genus are ignored, reducing the accuracy of driving factor determination. Moreover, the determination of driving factor thresholds is primarily based on water quality measurements following cyanobacterial blooms (Hu et al., 2010). Most cyanobacterial bloom prediction models based on these measurements are black-box models without clear mechanisms, such as genetic algorithms (Sivapragasam et al., 2010), Bayesian networks (Rigosi et al., 2015), and neural networks (Descy et al., 2016; Tao et al., 2017). Furthermore, most models rely on monitoring cyanobacterial bloom data, so they cannot be applied to areas where cyanobacterial blooms have not yet been detected (Giannuzzi et al., 2012; Zhao and Huang, 2014; Bukowska et al., 2017) or applied directly to other regions beyond the monitoring area. They also cannot effectively predict the range and time of cyanobacterial blooms, limiting our ability to predict and control blooms. Further studies are necessary to determine the dominant cyanobacterial species in a habitat and their principal driving factors, to establish versatile cyanobacterial bloom probability prediction models thereby, predicting the occurrence of cyanobacterial blooms globally.

The aims of this study were to present a versatile method to predict the occurrence of cyanobacterial blooms and determine the thresholds of bloom water quality driving factors, based on the dominant cyanobacterial species. We hypothesized that the water quality factors did not interact with each other, that is, a change in one factor did not directly lead to changes in other factors. We also expected that water quality would reflect the degree of eutrophication, and high eutrophication of a water body would lead to the outbreak of cyanobacterial blooms. The method from this study is user-friendly and could significantly enhance the prevention of cyanobacterial blooms globally, ensuring the health of aquatic ecosystems, drinking water, and humans.

## 2. Material and methods

### 2.1. Study area

Jinan or Spring City (36.0–37.5°N, 116.2–117.7°E) is a pilot city for the construction of a civilized and ecological city in China. It has a steeper topography in the South than in the North since it is bordered by Mount Tai in the South. The Yellow River traverses the city (Fig. 1). The altitude ranges from –30 to 937 m ASL, with highly contrasting relief. The average annual temperature is 14.3 °C, and the highest average

**Table 1**  
Driving factors of cyanobacteria blooms within the last 10 years from the literature.

Driving factors	Taxonomic level	Surroundings	Study area	References
Total phosphorus, water temperature	Genus	Farmland	Lake Beysehir, Turkey	Bucak et al., 2018
Total phosphorus, total nitrogen, water temperature	Genus	Farmland	Daechung Reservoir, Korea	Joung et al., 2011
	Genus	Aquaculture pond	A typical freshwater aquaculture pond, China	Hu et al., 2018
	Genus	Farmland	Baekje Reservoir, Korea	Park et al., 2017
	Genus	Farmland	A tropical lake, Brazil	Figueredo and Giani, 2009
	Genus	Farmland	Indian River Lagoon, Florida, USA	Phlips et al., 2011
	Genus	Farmland	Lake Taihu, China	Li et al., 2014 Duan et al., 2018
	Species	Farmland	Nansi Lake, China	Tian et al., 2013
Total phosphorus, total nitrogen, water temperature, turbidity	Genus	Farmland	Five shallow lakes, Europe	Descy et al., 2016
Total phosphorus, total nitrogen, water temperature, pH	Genus	Farmland	Cachoeira Dourada, Brazil	Teixeira de Oliveira et al., 2011
	Genus	Farmland	Maixi River estuary to the Baihua Reservoir, China	Li et al., 2013
Total phosphorus, total nitrogen, nitrate nitrogen, ammonia nitrogen	Genus	Farmland	Lake Erie, U.S./Canada	Steffen et al., 2017
Total phosphorus, total nitrogen, chemical oxygen demand	Genus	Farmland and town	Lake Dianchi, China	Hou et al., 2004
Total nitrogen/total phosphorus, nitrate nitrogen	Genus	Farmland and town	Ford Lake, Michigan, USA	Lehman et al., 2009
Water temperature, light intensity	Species	Farmland	Funil Reservoir, Brazil	Soares et al., 2009
Water temperature, pH, total phosphorus, turbidity	Genus	Farmland	Mundau reservoir, Brazil	Dantas et al., 2008
Water temperature, nitrate nitrogen, ammonia nitrogen	Genus	Farmland	Lake Chaohu, China	Cai and Kong, 2013
Total nitrogen, total phosphorus, total nitrogen/total phosphorus	Genus	Farmland	Lake Taihu, China	Xu et al., 2010
Total nitrogen, total phosphorus, dissolved oxygen, conductivity, water temperature	Genus	Farmland	Lake Erhai, China	Zhu et al., 2018
Total phosphorus, pH, water temperature, turbidity, nitrate nitrogen, light intensity	Genus	Farmland	Chaohu, China	Zhang et al., 2016
Water temperature, pH, total phosphorus, nitrate nitrogen, ammonia nitrogen	Genus	Farmland	Dashahe and Gaozhou Reservoirs, China	Yuan et al., 2015
	Genus	Farmland	Faxinal Reservoir, Brazil	Becker et al., 2009

monthly temperature is in July, ranging from 26.8 to 27.4 °C, while the lowest is in January, ranging from 1.4 to 3.2 °C (Cui et al., 2009; Zhang et al., 2010). Jinan City represents a typical developing city in China, with an area of 8227 km<sup>2</sup> and a population of 5.69 million (Zhang et al., 2007). With rapid industrial development and urbanization in recent decades, large amounts of nutrients flow into its lakes and reservoirs. Therefore, lakes and reservoirs are severely polluted, and the risk of cyanobacterial blooms is unprecedentedly high. As a result, drinking water and human health and well-being are increasingly being threatened (Hong et al., 2010). There are >30 lakes and reservoirs in Jinan, most with water supply functions. There is an urgent need to control cyanobacterial proliferation to prevent cyanobacteria bloom outbreaks and protect the drinking water and human health.

## 2.2. Data

Based on a comprehensive analysis of the characteristics of the watershed and river system of Jinan City, 13 reservoirs located in different tributaries and two typical lakes were selected for monitoring. In the spring, summer, and autumn of 2014 and 2015, six large-scale field investigations concurrently recorded a large quantity of water quality and biological data in the 15 lakes and reservoirs, to analyze the principal driving factors of cyanobacterial blooms and determine their threshold values.

### 2.2.1. Phytoplankton data

A 1 L organic glass bottle was used to sample water from 0 to 2 m below the water surface. As quickly as possible, a 1.5% concentration of Lugol's solution was added to the bottle. In the laboratory, a 24-h sedimentation method was used to concentrate the phytoplankton sample to 30 mL. To determine individual biovolume, individual size (length, height, and breadth or diameter) of a species was

measured using a plankton microscope. The average size of at least 50 individuals was used to calculate the average biovolume of a species (SL167-96<sup>1</sup>); for more details refer to Zhao et al. (2012).

### 2.2.2. Water quality data

In the six field investigations, 480 water samples were collected. All water quality parameters are listed in Table 2. The physical parameters were measured in situ with portable equipment and the chemical parameters were obtained by testing water samples in the laboratory within 24 h of collection from the monitoring stations. A spectrophotometer (DR5000), atomic absorption spectrophotometer (Thermo M6), and ion chromatograph (DIONEX-600) were used to measure chemical parameters; for more details refer to Zhao et al. (2015b).

## 2.3. Data analysis

### 2.3.1. Identification of dominant cyanobacterial species

We used a dominance model and the mutation point method to determine the dominant cyanobacterial species. The dominance model (Eq. (1) by Zhao et al., 2014) reflected the importance of both the abundance and biomass of a species to its community and avoided bias caused by using only abundance or biomass.

$$\begin{cases} I_{m,i} = \omega_1 P_{a,i} + \omega_2 P_{b,i} \\ P_{a,i} = \frac{N_i}{\sum N_i}, P_{b,i} = \frac{B_i}{\sum B_i} \end{cases}, \quad (1)$$

where  $I_m$  is the dominance of a cyanobacterial species;  $i$  is the  $i^{\text{th}}$  cyanobacterial species;  $P_a$  and  $P_b$  refer, respectively, to the ratios of the species' abundance and biomass to the total of the communities with consideration to the spatial presence/absence of the species;  $N_i$  is the abundance of the  $i^{\text{th}}$  cyanobacterial species and  $B_i$  is the biomass of the

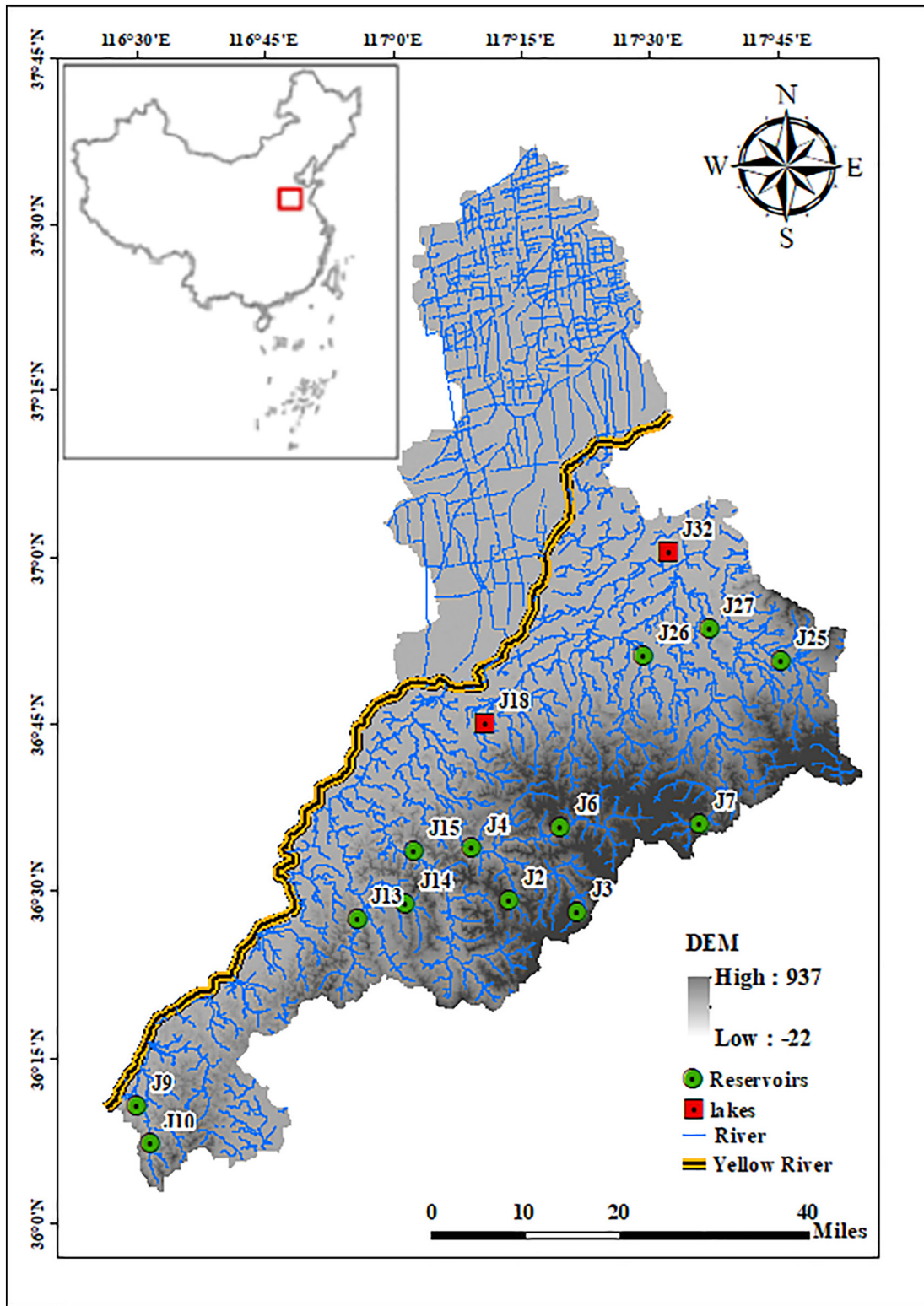


Fig. 1. Lakes and reservoirs of Jinan City and the suburban areas, showing locations of hydrology, water quality, and aquatic ecosystem monitoring stations.

species; and  $\omega_1$  and  $\omega_2$  are the weightings of abundance and biomass, respectively.

$$\begin{cases} \frac{\omega_1}{\omega_2} = \frac{a}{b} \\ \omega_1 + \omega_2 = 1.0 \end{cases} \quad (2)$$

where  $a$  and  $b$  are the positions of the centroid in the one-dimensional

coordinates  $P_a$  and  $P_b$ ;  $a$  and  $b$  can be determined using the density function of the mass systems, which can be rewritten in this study as follows:

$$\begin{cases} a = \frac{\sum P_{a,i} N_i}{\sum N_i} \\ b = \frac{\sum P_{b,i} B_i}{\sum B_i} \end{cases} \quad (3)$$



**Table 2**Physical and chemical environmental parameters included in the Jinan City monitoring program (the numbers in parenthesis indicate mean  $\pm$  SD) (Zhao et al., 2015a).

Parameter	Name	Abbreviation	Unit	Range (mean $\pm$ SD)
Physical	Air temperature	AT	°C	15.0–33.1 (20.3 $\pm$ 4.6)
	Water temperature	WT	°C	16.70–30.60 (19.8 $\pm$ 2.85)
	pH	pH		7.26–8.60 (7.84 $\pm$ 0.35)
	Conductivity	Cond	mS/m	326–4130 (2132.1 $\pm$ 913)
	Transparency	Trans	Cm	0–600 (352.21 $\pm$ 111.32)
	Turbidity	Turb	Degree	0.52–924 (432.42 $\pm$ 139.53)
Chemical	Calcium	Ca	mg L <sup>-1</sup>	17.63–315.83 (123.54 $\pm$ 58.39)
	Chlorine	Cl	mg L <sup>-1</sup>	11.85–786.15 (345.68 $\pm$ 176.39)
	Sulfate	SO <sub>4</sub>	mg L <sup>-1</sup>	43.47–932.22 (462.58 $\pm$ 179.28)
	Carbonate	CO <sub>3</sub>	mg L <sup>-1</sup>	0–12.50 (6.54 $\pm$ 2.83)
	Bicarbonate	HCO <sub>3</sub>	mg L <sup>-1</sup>	50.05–845.32 (357.68 $\pm$ 132.11)
	Total alkalinity	TA	mg L <sup>-1</sup>	51.48–693.35 (235.87 $\pm$ 107.60)
	Total hardness	TH	mg L <sup>-1</sup>	141.12–989.59 (532.12 $\pm$ 198.71)
	Dissolved oxygen	DO	mg L <sup>-1</sup>	1.17–9.92 (5.61 $\pm$ 2.41)
	Total nitrogen	TN	mg L <sup>-1</sup>	0.25–21.84 (5.68 $\pm$ 4.18)
	Ammonia	NH <sub>4</sub> -N	mg L <sup>-1</sup>	0.07–9.42 (3.54 $\pm$ 2.63)
	Nitrite	NO <sub>2</sub>	mg L <sup>-1</sup>	0–1.41 (0.87 $\pm$ 0.30)
	Nitrate	NO <sub>3</sub>	mg L <sup>-1</sup>	0.05–18.85 (10.57 $\pm$ 2.90)
	Permanganate index	COD_Mn	mg L <sup>-1</sup>	0.57–16.36 (5.63 $\pm$ 3.34)
	Biochemical oxygen demand	BOD	mg L <sup>-1</sup>	0–35.80 (15.28 $\pm$ 7.39)
	Total phosphorus	TP	mg L <sup>-1</sup>	0–3.64 (1.69 $\pm$ 0.78)
	Fluoride	Fluoride	mg L <sup>-1</sup>	0.18–2.30 (1.37 $\pm$ 0.49)

The other 10 heavy metal ions, e.g., copper, zinc, and lead, were below detection levels, and have not been included in the above table.

Eqs. (2), (3) are used to determine weightings in Eq. (1) in this paper (Zhao et al., 2015b).

After the dominance indices of all species were calculated, the dominant species of the biological community were identified by the breakpoint (i.e., the point on the dominance curve where the curvature was significantly smaller after that point than the curvature before) was determined based on curvature of cumulative dominance using Eq. (4) (Gippel and Stewardson, 1998; Zhao et al., 2015b).

$$K = \frac{d^2y}{dx^2} \left[ 1 + \left( \frac{dy}{dx} \right)^2 \right]^{-\frac{3}{2}} \quad (4)$$

where  $K$  represents the curvature of the dominance curve. This method selects the dominant species in the aquatic population objectively.

### 2.3.2. Determination of principal driving factors by CCA

We used CCA to determine the principal driving factors of the dominant cyanobacterial species. Canonical correspondence analysis (CCA) is a multivariate gradient analysis method designed to elucidate relationships between biological assemblages of species and water quality factors and has been widely used to predict interactions between community structure and environmental variables (Godoy et al., 2002; Martino and Able, 2003; Biswas et al., 2014). It requires two data matrices, which were the species and environmental data matrices in this study. Habitat factors influencing cyanobacterial communities included physical and chemical water quality parameters.

Detrended canonical analysis (DCA) is an analytical method for species and environmental factors similar to CCA. It is often used to test the “arc effect” before using CCA (Palmer, 1993). If the gradient of the first axis in DCA is large, the species responses can be assumed to be unimodal and CCA can be used without the “arc effect” (Lepš and Šmilauer, 2003). Otherwise, other analytical methods have to be used. In this way, the impact of the “arc effect” on the analytical method can be minimized.

We used DCA before the CCA in the present study; the gradient of the first axis was long, so CCA was the appropriate analytical method. Methods using unimodal ordination with a Monte Carlo permutation test were used to select principal factors ( $p < 0.05$ ) from the three

forementioned parameters that underpinned the spatial heterogeneity of the cyanobacterial communities. The figures of CCA were drawn using Canoco 4.5.

In the CCA ordination map, the arrowed lines represented environmental factors. The biplot scores of each environmental factor indicated its impact on the biomes. The larger the biplot scores, the greater the impact. The more the absolute value of the cosine of the angle between a species and an environmental factor is closer to 1, the closer the relationship between the species and the environmental factor. Thus, the principal driving factors of the biomes can be selected.

### 2.3.3. Calculation of cyanobacterial bloom occurrence probability

We proposed a new cyanobacterial bloom occurrence prediction model to compensate for the shortcomings of the previous bloom prediction models and quantitatively calculate the risk of cyanobacterial bloom outbreaks and thresholds of principal driving factors. The occurrences of cyanobacterial blooms were affected by numerous water quality factors. Under field conditions, the effects of individual water quality factors on cyanobacterial populations are difficult to isolate (Wu et al., 2016). Although the effects can be studied using laboratory cultures with controlled variables (Moller et al., 2014), the application of research results is limited to specific algal species and water quality factors. Moreover, the effects of the same factors on cyanobacteria have significant gaps in different environmental conditions (Spencer et al., 2011). Therefore, previous cyanobacterial bloom prediction models have previously been based on black-box models, such as neural networks (Descy et al., 2016). However, these models heavily rely on machine learning, and their accuracy requires an excessive quantity and quality of data during and after blooms (Tao et al., 2017). Consequently, these types of models cannot analyze outbreak risks and critical environmental driving factors without cyanobacterial blooms.

In this study, the effects of various water quality factors on cyanobacterial populations were separated and quantified based on the previous screening of dominant cyanobacterial species and the determination of principal driving factors. If all driving factors were in their optimized value ranges, the cyanobacterial bloom outbreaks were likely to occur. The closer the measured values of driving factors were to their optimized values, the higher the probability of cyanobacterial bloom occurrence. A cyanobacterial bloom occurrence probability (P) prediction model was thus, established (Eqs. (5) and (6)) in combination with the results of the principal driving factors, to

determine the risk of occurrence and principal driving factor thresholds under conditions of no cyanobacterial blooms.

$$P = 1 - \sum_{i=1}^n a_i \left( \frac{|X_i - X_i^b|}{X_i^b} \right) \quad (5)$$

and

$$\sum_{i=1}^n a_i = 1, \quad (6)$$

where  $P$  represents the probability of a cyanobacterial bloom;  $n$  is the number of principal driving factors;  $a_i$  is the weight of the  $i^{\text{th}}$  driving factor;  $X_i$  is the measured value of the  $i^{\text{th}}$  driving factor, and  $X_i^b$  is the optimum value of the  $i^{\text{th}}$  driving factor.

The values of  $a_i$  were determined by the biplot scores in CCA sorting. If the first canonical axis explained the relationship between environmental variables and species, then the  $a_i$  value was normalized based on the absolute values of the biplot scores on the first canonical axis of each environmental variable. If the first canonical axis could not explain the relationship between environmental variables and species, then the root mean square of the biplot scores in both the first and second canonical axis was normalized to obtain the  $a_i$  value.

The values of  $X_i^b$  were determined using the habitat suitability index (HSI). Habitat suitability is defined as the preference of an aquatic organism for a particular set of habitat attributes (Vadas and Orth, 2001; Vismara et al., 2001). It is widely used to indicate the degree of preference of species for different habitats (Leclerc et al., 2003; Ahmadi-Nedushan et al., 2006). It varies between 0 and 1, and a higher HSI value indicates a more suitable habitat (Bovee, 1998). The value range of each driving factor, from the minimum to maximum, were classified into five levels of sub-ranges to plot the HSI graph. The range of the maximum HSI was then selected as the optimum range of the driving factor, and the median value of this range was taken for  $X_i^b$ , the optimum value of this driving factor.

### 3. Results

#### 3.1. Dominant cyanobacterial species

A total of 141 phytoplankton species belonging to 8 phyla, 10 classes, 13 orders, 27 families, and 29 genera were collected from 90 stations in

the six large-scale field investigations. Based on these species, dominant cyanobacterial species were determined using Eqs. (1)–(3). In Eq. (1), the weights of abundance and biomass,  $\omega_1$  and  $\omega_2$ , were 0.67 and 0.33, with which species dominance values were then calculated. After sorting the dominance from large to small and calculating the degree of accumulation, the dominance curve was plotted (Fig. 2). The mutation point was then calculated from the dominance curve as (6, 0.902). Six species before the mutation point were then selected as dominant in the cyanobacterial population including, *Phormidium tenue* (SP17), *Oscillatoria tenuis* (SP15), *Microcystis aeruginosa* (SP10), *Merismopedia tenuissima* (SP13), *Raphidiopsis sinensis* (SP19), and *Merismopedia glauca* (SP18).

#### 3.2. Principal driving factors and cyanobacterial bloom probability prediction

The interpretation percentage of species–environment relation on the first canonical axis (horizontal axis in Fig. 3) reached 65.3% in Fig. 3a and 59.4% in Fig. 3b, indicating that the first axis could explain the relationship between environmental variables and species. So we could choose the principal driving factors based on the biplot scores of each environmental factor on the first canonical axis. The results of CCA showed that the principal physical water quality factors affecting the distribution of dominant cyanobacterial species in Jinan were water temperature (WT) and pH; the principal chemical water quality factors were total phosphorus (TP), ammonia nitrogen ( $\text{NH}_4\text{-N}$ ), chemical oxygen demand (COD), and dissolved oxygen (DO) (Fig. 3). SP10, SP13, SP15, and SP18 are significantly affected by WT. In addition, TP significantly affected SP15, SP17, and SP18, in a similar manner as  $\text{NH}_4\text{-N}$  and DO; whereas, SP10 and SP13 were significantly affected by COD.

All the principal driving factors mentioned above, along with dominant cyanobacteria identified, were used for further CCA analyses (Fig. 4a) to determine the weights of the driving factor. The interpretation percentage of the species–environment relation reached 63.5% on the first canonical axis, so the biplot scores on the first canonical axis could represent the impact of environmental factors on species. The absolute values of biplot scores on the first axis for WT, pH, TP,  $\text{NH}_4\text{-N}$ , COD, and DO were 0.673, 0.311, 0.488, 0.875, 0.927, and 0.946, respectively. After the values were normalized, weights  $a_i$  in Eq. (5) for WT, pH, TP,  $\text{NH}_4\text{-N}$ , COD, and DO were as 0.179, 0.082, 0.129, 0.232, 0.246, and 0.132, respectively.

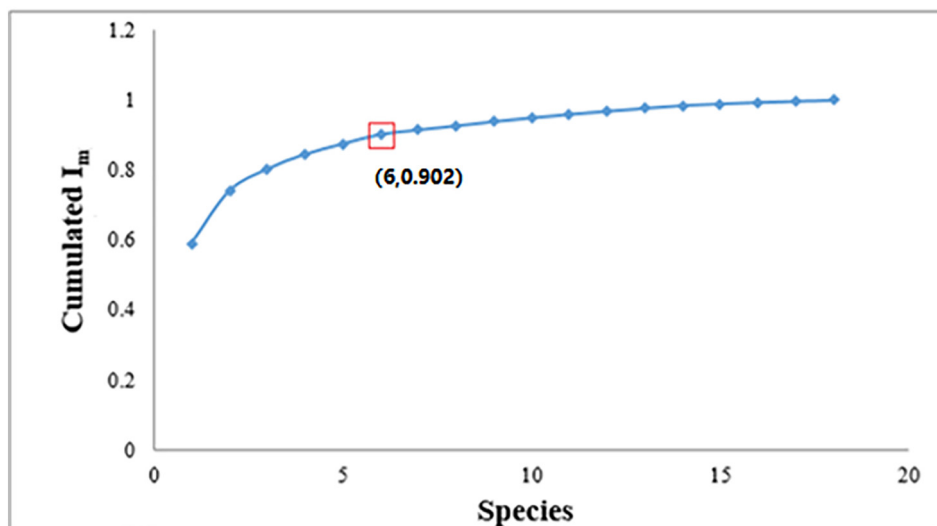
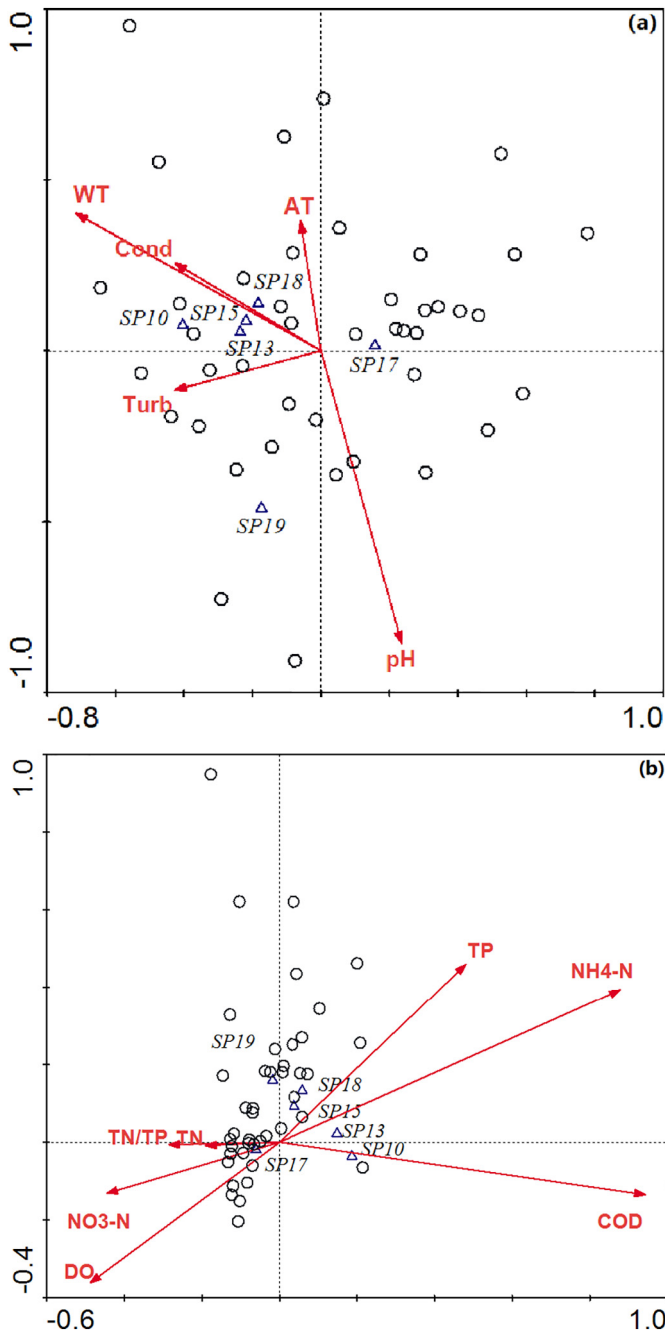


Fig. 2. Mutation point of dominance index for cyanobacteria in lakes and reservoirs, determined using Eq. (4).



**Fig. 3.** Canonical correspondence analysis of biological and water quality factors at monitoring stations located in reservoirs and lakes in 2014–2015 (the abbreviations of parameters are listed in Table 2. (a): Physical water quality factors, (b): Chemical water quality factors).

The five levels of the parameters were determined according to the ranges in Table 3. The HSI value of each fraction was calculated to determine the HSI graphs (Fig. 5), which indicated that the optimum values ( $X_i^0$  in Eq. (5)) of WT, pH, TP,  $\text{NH}_4\text{-N}$ , COD, and DO were 26 °C, 7.5, 0.175 mg L<sup>-1</sup>, 0.5 mg L<sup>-1</sup>, 14 mg L<sup>-1</sup>, and 6.62 mg L<sup>-1</sup>, respectively.

Values of  $a_i$  and  $X_i^0$  were then used to calculate the occurrence probability (P) of cyanobacterial blooms at each monitoring station with Eq. (5). The probability (P) of a cyanobacterial outbreak was plotted as the x-axis, and the cumulative density (C) of cyanobacteria was plotted as the y-axis (P-C relation, Fig. 4b). When the P value exceeded 0.70–0.80, the density increased rapidly with increases in P.

An exponential function for the P-C relation was then fitted as  $y = 2.5698e^{10.4895x}$  ( $R^2 = 0.9237$ ). Levene's test for equality of variances

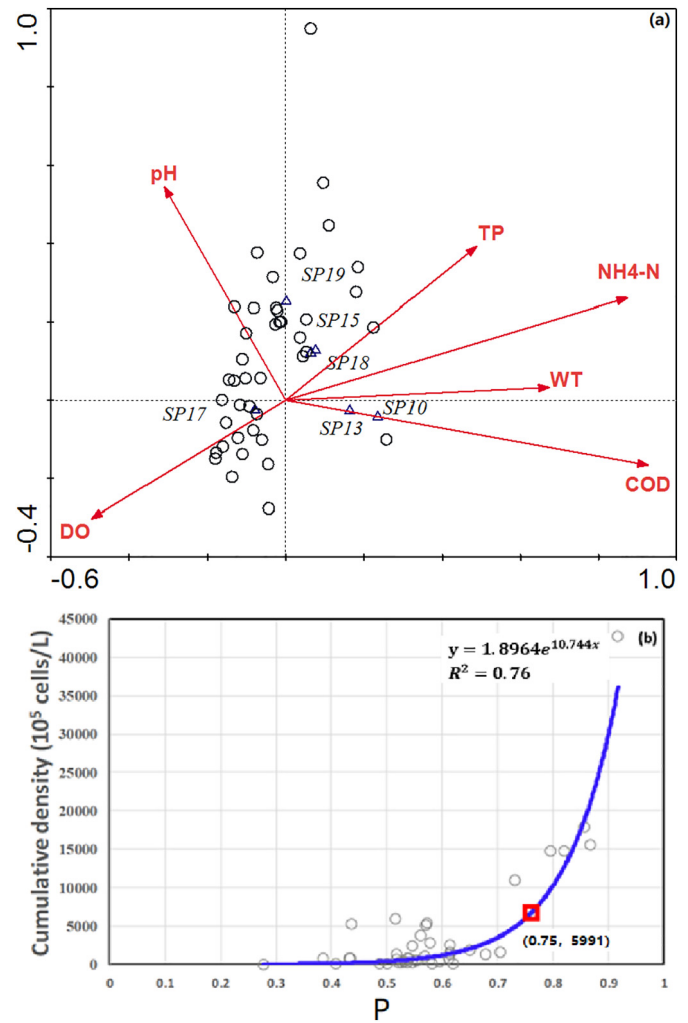


**Fig. 4.** Changing of bloom probability with dominant cyanobacterial species density. (a) Canonical correspondence analysis of principal driving factors for weight determination; (b) Relationship between the probability of blooms (P) and cumulative density of cyanobacteria (C). Points where P is >0.75 (red box) represent summer samplings at the two stations J7 and J13. (For interpretation of the references to color in this figure legend, the reader is referred to the web version of this article.)

revealed that simulated C had the same distribution as that of the observed C ( $F = 0.49$ ,  $p > 0.05$ ), indicating that the simulated and observed C data sets had homogeneity of variance. Furthermore, the paired-samples *t*-test revealed that the means of the two data sets were equal at a significance level of 5% ( $t = 0.261$ ,  $p > 0.05$ ). According to the mutation point identification model in Zhao et al. (2015b), the second derivative was calculated for the fitting equation, indicating that the curvature of the curve changed significantly before and after  $P = 0.75$ , which was then taken as the point of mutation (shown in the red box in Fig. 4b). When  $P > 0.75$ , all the principal driving factors were within their optimal range, therefore cyanobacteria rapidly proliferated, further increasing the risk of a cyanobacterial bloom.

Fig. 4b shows that the P-value of each point does not vary considerably over time. The spatial distribution figure (Fig. 6) was made using the mean value of P at each point.

#### 4. Discussion

##### 4.1. Verification and comparison of dominant species in other areas

Among the six selected dominant species, *P. tenue* had the most dominant cyanobacterial populations in lakes and reservoirs of Jinan,

**Table 3**  
Levels of principal driving factors.

Level	1	2	3	4	5
WT (°C)	12.00–16.00	16.00–20.00	20.00–24.00	24.00–28.00	28.00–32.00
pH	7.30–7.70	7.70–8.10	8.10–8.50	8.50–8.90	8.90–9.30
TP (mg L <sup>-1</sup> )	0–0.05	0.05–0.10	0.10–0.15	0.15–0.20	0.20–0.25
NH <sub>4</sub> -N (mg L <sup>-1</sup> )	0–0.20	0.20–0.40	0.40–0.60	0.60–0.80	0.80–1.00
COD (mg L <sup>-1</sup> )	2.30–4.90	4.90–7.50	7.50–10.10	10.10–12.70	12.70–15.30
DO (mg L <sup>-1</sup> )	2.40–4.09	4.09–5.77	5.77–7.46	7.46–9.14	9.14–10.83

with a relatively wide niche, and could adapt to a wide range of environmental conditions (Li et al., 2017), making it regularly prone to blooms (Meng et al., 2013). *Oscillatoria tenuis* and *M. aeruginosa* are common bloom algae and can produce harmful algal toxins (Huang et al., 2008; Bouhaddada et al., 2016), and *M. tenuissima* and *M. glauca* are common bloom algae at higher water temperatures and low turbulence

conditions (Tian et al., 2014). These algae are also the focus of studies on cyanobacterial blooms in other regions of China and around the world (Marshall, 2009; Zhang et al., 2011; Tian et al., 2013; Bouhaddada et al., 2016; Park et al., 2017; Chen et al., 2018; Duan et al., 2018). Studies from Asia (Jiang et al., 2017; Liu and Fang, 2017), North America (Werner et al., 2012; Carmichael and Boyer, 2016),

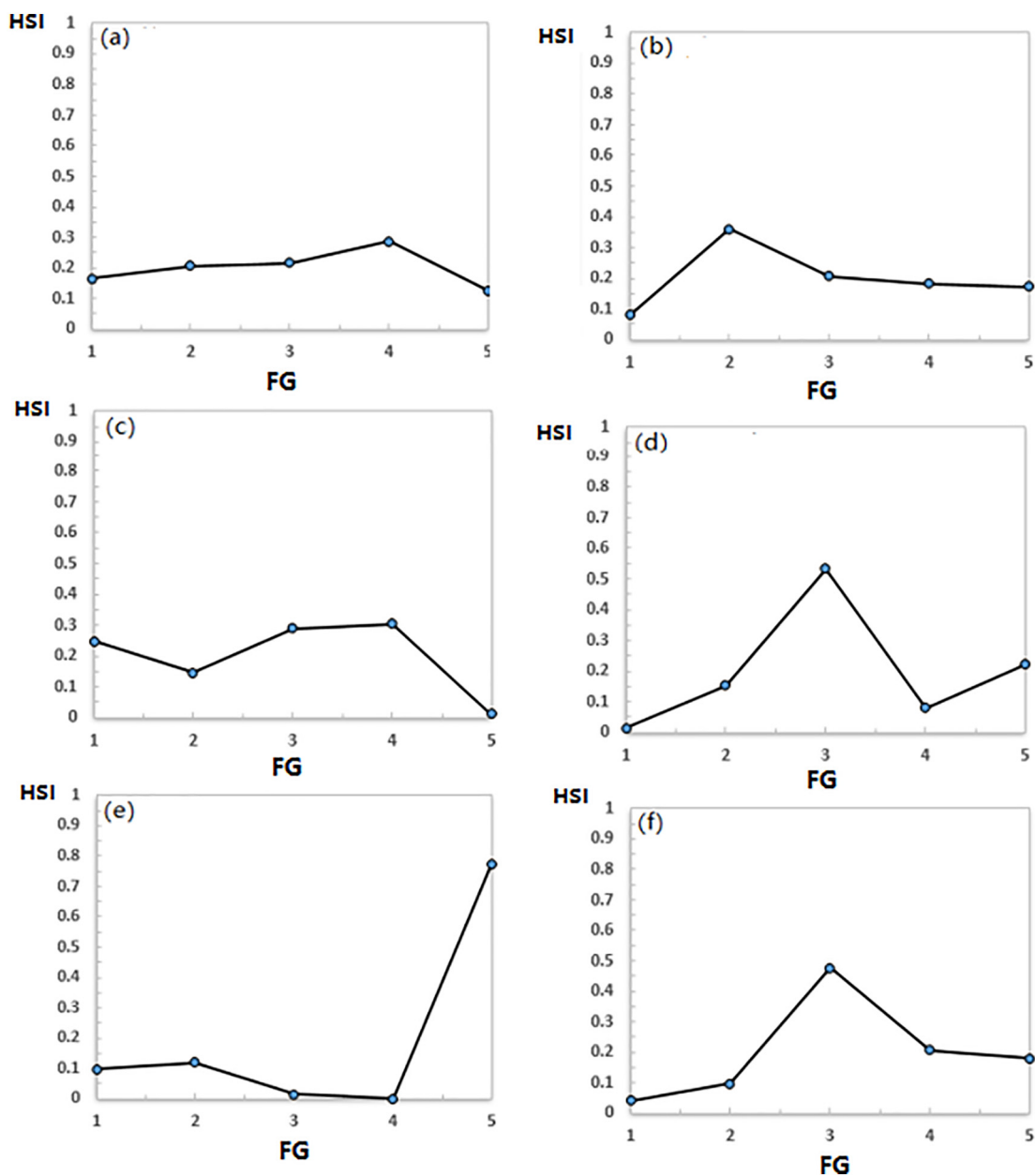


**Fig. 5.** Habitat suitability index (HSI) graphs of each principal driving factor. X-axis are factor gradient and y-axis are habitat suitability index. (a) WT, (b) pH, (c) TP, (d) NH<sub>4</sub>-N, (e) COD, (f) DO.



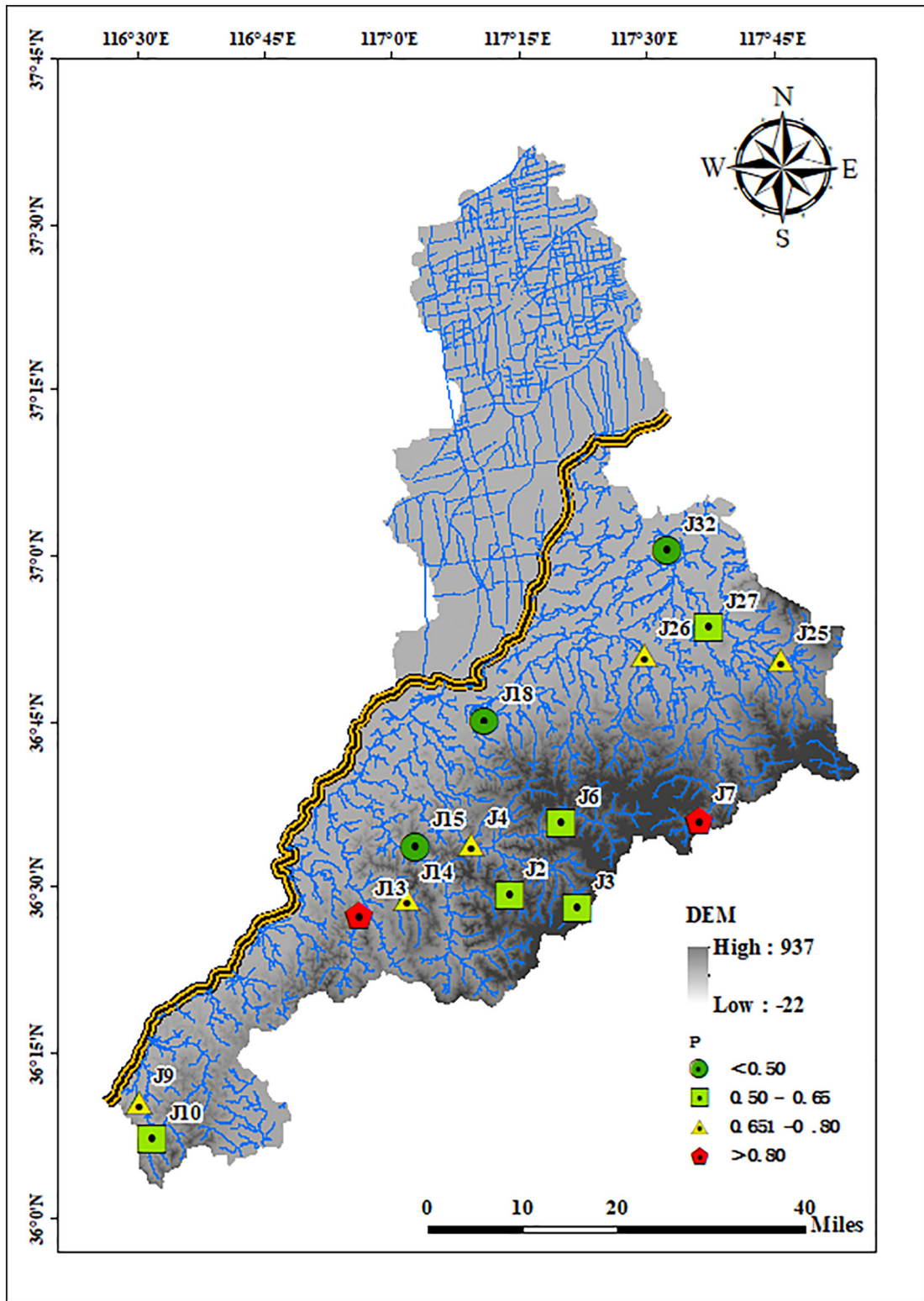


Fig. 6. Probability spatial distribution map of cyanobacterial blooms.

South America (Lins et al., 2016), and Europe (Funari et al., 2017; Scherer et al., 2017; Burak et al., 2018) show that cyanobacteria have distinct physiological characteristics that make them dominant in algae competition and able to easily form cyanobacterial blooms (Hu, 2011; Xiao et al., 2012). Therefore, the predictive analysis of cyanobacterial blooms using these algae as dominant species probably represents the actual conditions of the algal populations in Jinan City. Thus, our results are representative of field conditions, universal, and

suitable for use in lakes and reservoirs globally with similar dominant species.

#### 4.2. Rationality analysis of driving factors

The CCA analysis showed that the major water quality physical factors that drove the dominant cyanobacterial population in Jinan City were WT and pH. Cyanobacteria-favored WT accelerated cyanobacterial

reproduction (Moller et al., 2014; Sinden and Sinang, 2016; Bertani et al., 2017), with water temperature being the most important physical driving factor for cyanobacterial blooms (Figueredo and Giani, 2009; Descy et al., 2016; Hu et al., 2018). Cyanobacterial growth and reproduction is dependent on an alkaline environment (Cremona et al., 2018). Acidic waters have a low pH, which can limit the outbreak of cyanobacterial blooms (Dantas et al., 2008; Teixeira de Oliveira et al., 2011). In addition, the driving water quality chemical factors included, TP, NH<sub>4</sub>-N, COD, and DO, where TP and NH<sub>4</sub>-N were the main indicators of eutrophication and essential for algal growth and reproduction (Becker et al., 2009; Steffen et al., 2017). Appropriate concentrations of COD and DO promote rapid cyanobacterial growth (Hou et al., 2004; Zhu et al., 2018). In previous studies, in addition to the above factors, TN, Turb, N/P, etc. were also considered major environmental drivers of cyanobacterial blooms (Dantas et al., 2008; Xu et al., 2010). However, in this study, the temporal and spatial changes in TN and Turb were not significant, and their driving effect was not evident. This further led to a small temporal and spatial change in N/P, and they were excluded as principal driving factors. These results showed that the size of the study area and temporal and spatial scales of phytoplankton sampling were the major factors affecting the selection of driving factors.

#### 4.3. Determination of thresholds for cyanobacteria bloom driving factors

When the P value exceeded 0.75, the principal driving factors were in their optimum range, and the cyanobacteria proliferated rapidly (Kovacs et al., 2012; Wood et al., 2017). The greater the P value, the higher the density of cyanobacteria, and the greater the risk of cyanobacterial blooms (Leão et al., 2009; Maske et al., 2010). This further validated the rationality of the cyanobacterial bloom probability model proposed in this study, which could therefore effectively inform the management of lakes and reservoirs globally to control the development of cyanobacteria.

Regarding WT, Pang et al. (2013) showed that when it ranged from 20 to 28 °C, *Microcystis* had rapid growth and mortality rates in Taihu Lake, China. Beaulieu et al. (2013) analyzed data from 1000 lakes across the United States and concluded that algae were more likely to grow in warmer water (approximately 25 °C), which was within the range of WT thresholds obtained in this study. For pH, because cyanobacterial growth and reproduction depends on the alkalinity of an environment (Cremona et al., 2018) our pH calculations (5.63–9.38) were adjusted to the range 7–9.38. Similarly, Burak et al. (2018) conducted studies in Süloğlu Reservoir, Turkey, and their results showed that the pH for the cyanobacterial bloom environment ranged from 7.73 to 9.25. Furthermore, Yang et al. (2018a, 2018b) showed that cyanobacteria had a competitive advantage in a pH range of 7–9 indoors.

Total phosphorus and NH<sub>4</sub>-N are nutritive substances, and previous studies did not establish threshold ranges. Data analyses conducted by Dai et al. (2015) and Steffen et al. (2017) in Lake Poyang, China and Lake Erie, North America, respectively, showed that cyanobacteria were at a higher density within the TP and NH<sub>4</sub>-N ranges in this study. Moreover, according to the indoor cultivation results from Duan et al. (2018), the cyanobacterial growth rate was also high within this range, indicating that this was a reasonable threshold range. Similar to our findings, Yang et al. (2018a, 2018b) showed that COD was the most important environmental factor affecting the cyanobacterial communities in Dianchi Lake, China, with a range of 9.81–15.0 mg L<sup>-1</sup>. The results of Carneiro (2014) from different tributaries of the Rio Verde Lake watershed in Brazil indicated that during cyanobacterial blooms, the COD values of most tributaries were approximately 11.0 mg L<sup>-1</sup>, within the COD threshold range obtained here. Similar to our results, Zhu et al. (2018) showed that the DO content was 5.40–8.66 mg L<sup>-1</sup> in Lake Erhai, China during the season when cyanobacteria had a high bio-density. In addition, Park et al. (2018) showed that the DO concentration was mostly at 5.0–8.0 mg L<sup>-1</sup> during the high cyanobacterial

bio-density period in Hoedong Reservoir, South Korea. The results from these global studies have further validated the principal driving factor thresholds of cyanobacterial blooms stated in this paper, strongly indicating that our method has great potential to be extrapolated to the global risk prediction of cyanobacterial blooms.

## 5. Conclusions

In this study, a cyanobacterial bloom probability model was proposed to calculate the probability of cyanobacterial bloom outbreaks. Through applications in Jinan City, we found that when the probability of cyanobacterial blooms exceeded 0.75, cyanobacteria proliferated rapidly, which further increased the risk of cyanobacterial blooms. Threshold ranges of the principal driving factors for cyanobacterial blooms in the study area were WT: 19.5–32.5 °C, pH: 7–9.38, TP: 0.13–0.22 mg L<sup>-1</sup>, NH<sub>4</sub>-N: 0.38–0.63 mg L<sup>-1</sup>, COD: 10.5–17.5 mg/L, and DO: 4.97–8.28 mg L<sup>-1</sup>. The results from studies in other regions of the world further validated the driving factor thresholds mentioned above and provided evidence that the proposed model could be extended to other regions of the world.

## Acknowledgments

We acknowledge the reviewers and editors for their valuable advice on improving the quality of this paper. We thank the China Scholar Council (CSC) and our colleagues from Dalian Ocean University, Jinan and Dongying Survey Bureau of Hydrology, and Beijing Normal University for their support in funding the research and collaboration during field investigations.

This research was jointly supported by the National Natural Science Foundation Program of China (grant numbers: u1812401 & 41471340), the 111 Project (B18006), the National Key Project for R&D (grant numbers: 2016YFC0402403 & 2016YFC0402409), and the Shaanxi Key Science and Technology Innovation Team Project (grant number: 2014KCT-27), China.

## References

- Ahmadi-Nedushan, B., St-Hilaire, A., Bérubé, M., Robichaud, É., Thiémonge, N., Bobée, B., 2006. A review of statistical methods for the evaluation of aquatic habitat suitability for instream flow assessment. *River Res. Appl.* 22 (5), 503–523.
- Arhonditsis, G.B., Brett, M.T., 2005. Eutrophication model for Lake Washington (USA): part I. Model description and sensitivity analysis. *Ecol. Model.* 187 (2–3), 140–178.
- Beaulieu, M., Pick, F., Gregory-Eaves, I., 2013. Nutrients and water temperature are significant predictors of cyanobacterial biomass in a 1147 lakes data set. *Limnol. Oceanogr.* 58 (5), 1736–1746.
- Becker, V., Huszar, V.L.M., Crossetti, L.O., 2009. Responses of phytoplankton functional groups to the mixing regime in a deep subtropical reservoir. *Hydrobiologia* 628 (1), 137–151.
- Bertani, I., Steger, C.E., Obenour, D.R., Fahnenstiel, G.L., Bridgeman, T.B., Johengen, T.H., et al., 2017. Tracking cyanobacteria blooms: do different monitoring approaches tell the same story. *Sci. Total Environ.* 575, 294–308.
- Biswas, S., Hussain, K.J., Das, N.P.I., Russell, B.C., Satpathy, K.K., Mishra, S.S., 2014. Imprint of monsoonal patterns on the fish assemblage in coastal waters of south-east India: a case study. *J. Fish Biol.* 85 (3), 773–799.
- Blomqvist, P., Pettersson, A., Hyenström, P., 1994. Ammonium-nitrogen—a key regulatory factor causing dominance of non-nitrogen-fixing cyanobacteria in aquatic systems. *Arch. Hydrobiol.* 132 (2), 141–164.
- Bouhaddada, R., Néliu, S., Nasri, H., Delarue, G., Bouaïcha, N., 2016. High diversity of microcystins in a *Microcystis* bloom from an Algerian lake. *Environ. Pollut.* 216, 836–844.
- Bovee, K., 1998. Stream habitat analysis using the instream flow incremental methodology. USGS, Biological Resources Division Information and Technology Report, pp. 1–131.
- Brookes, J.D., Carey, C.C., 2011. Resilience to blooms. *Science* 334 (6052), 46–47.
- Bucak, T., Trolle, D., Tavşanoğlu, Ü.N., Çakıroğlu, A.I., Özen, A., Jeppesen, E., et al., 2018. Modeling the effects of climatic and land use changes on phytoplankton and water quality of the largest Turkish freshwater lake: Lake Beyşehir. *Sci. Total Environ.* 621, 802–816.
- Bukowska, A., Kaliński, T., Koper, M., Kostrzewska-Szlakowska, I., Kwiatowski, J., Mazur-Marcz, H., Jasser, I., 2017. Predicting blooms of toxic cyanobacteria in eutrophic lakes with diverse cyanobacterial communities. *Sci. Rep.* 7 (1), 8342.
- Burak, O., Belgin, C.E., Salih, M.A., 2018. Influence of environmental conditions on the phytoplankton community assemblages in Süloğlu Reservoir (Edirne, Turkey). *Turk. J. Fish. Aquat. Sci.* 18, 969–982.

- Cai, Y., Kong, F., 2013. Diversity and dynamics of picocyanobacteria and the bloom-forming cyanobacteria in a large shallow eutrophic lake (Lake Chaohu, China). *J. Limnol.* 72 (3), 38.
- Carmichael, W.W., Boyer, G.L., 2016. Health impacts from cyanobacteria harmful algae blooms: implications for the North American Great Lakes. *Harmful Algae* 54, 194–212.
- Carneiro, C., 2014. Interpretative matrices approach to ranking lake sub-basin pollution potential: an applied study in Brazil. *Environ. Earth Sci.* 72 (5), 1697–1705.
- Chen, M.S., Ding, S.M., Chen, X., Sun, Q., Fan, X.F., Lin, J., et al., 2018. Mechanisms driving phosphorus release during algal blooms based on hourly changes in iron and phosphorus concentrations in sediments. *Water Res.* 133, 153–164.
- Cremona, F., Tuvikene, L., Haberman, J., Nöges, P., Nöges, T., 2018. Factors controlling the three-decade long rise in cyanobacteria biomass in a eutrophic shallow lake. *Sci. Total Environ.* 621, 352–359.
- Cui, B.S., Wang, C.F., Tao, W.D., You, Z.Y., 2009. River channel network design for drought and flood control: a case study of Xiaqinghe River basin, Jinan City, China. *J. Environ. Manag.* 90 (11), 3675–3686.
- Dai, G.F., Zhang, W., Peng, N.Y., Lou, Q., Zhong, J.Y., 2015. Study on distribution of N and P pollutants and risk of cyanobacteria bloom in Poyang Lake and waters around the lake during drought periods. *Ecol. Environ. Sci.* 24 (5), 838–844.
- Dalu, T., Wasserman, R.J., 2018. Cyanobacteria dynamics in a small tropical reservoir: understanding spatio-temporal variability and influence of environmental variables. *Sci. Total Environ.* 643, 835–841.
- Dantas, É.W., Moura, A.D.N., Bittencourt-Oliveira, M.D.C., Arruda Neto, J.D.D.T., Cavalcanti, A.D.D.C., 2008. Temporal variation of the phytoplankton community at short sampling intervals in the Mundaú reservoir, Northeastern Brazil. *Acta Bot. Bras.* 22 (4), 970–982.
- Descy, J.P., Leprieux, F., Pirlot, S., Leporcq, B., Van Wichelen, J., Peretyatko, A., et al., 2016. Identifying the factors determining blooms of cyanobacteria in a set of shallow lakes. *Ecol. Inform.* 34, 129–138.
- Duan, Z.P., Tan, X., Parajuli, K., Upadhyay, S., Zhang, D.F., Shu, X.Q., et al., 2018. Colony formation in two *Microcystis* morphotypes: effects of temperature and nutrient availability. *Harmful Algae* 72, 14–24.
- Eom, H., Borgatti, D., Paerl, H.W., Park, C., 2017. Formation of low-molecular-weight dissolved organic nitrogen in pre-denitrification biological nutrient removal systems and its impact on eutrophication in coastal waters. *Environ. Sci. Technol.* 51 (7), 3776–3783.
- Espie, G.S., Miller, A.G., Birch, D.G., Canvin, D.T., 1988. Simultaneous transport of CO<sub>2</sub> and HCO<sub>3</sub><sup>-</sup> by the cyanobacterium *Synechococcus* UTEX 625. *Plant Physiol.* 87 (3), 551–554.
- Figueredo, C.C., Giani, A., 2009. Phytoplankton community in the tropical lake of Lagoa Santa (Brazil): conditions favoring a persistent bloom of *Cylindrospermopsis* raciborskii. *Limnologia* 39 (4), 264–272.
- Funari, E., Manganelli, M., Buratti, F.M., Testai, E., 2017. Cyanobacteria blooms in water: Italian guidelines to assess and manage the risk associated to bathing and recreational activities. *Sci. Total Environ.* 598, 867–880.
- Giannuzzi, L., Carvajal, G., Corradini, M.G., Araujo Andrade, C., Echenique, R., Andrinolo, D., 2012. Occurrence of toxic cyanobacterial blooms in Rio de la Plata Estuary, Argentina: field study and data analysis. *Int. J. Toxicol.* 2012.
- Gippel, G.J., Stewardson, M.J., 1998. Use of wetted perimeter in defining minimum environmental flows. *Regul. Rivers Res. Manag.* 14 (1), 53–67.
- Godoy, E.A., Almeida, T.C., Zalmon, I.R., 2002. Fish assemblages and environmental variables on an artificial reef north of Rio de Janeiro, Brazil. *ICES J. Mar. Sci.* 59 (suppl), S138–S143.
- Havens, K.E., Fukushima, T., Xie, P., Iwakuma, T., James, R.T., Takamura, N., et al., 2001. Nutrient dynamics and the eutrophication of shallow lakes Kasumigaura (Japan), Donghu (PR China), and Okeechobee (USA). *Environ. Pollut.* 111 (2), 263–272.
- Hong, Q., Meng, Q.B., Wang, P., Wang, H.Y., Liu, R.M., 2010. Regional aquatic ecological security assessment in Jinan, China. *Aquat. Ecosyst. Health* 13 (3), 319–327.
- Hou, G.X., Song, L.R., Liu, J.T., Xiao, B.D., Liu, Y.D., 2004. Modeling of cyanobacterial blooms in hypereutrophic Lake Dianchi, China. *J. Freshw. Ecol.* 19 (4), 623–629.
- Hu, H.J., 2011. *Cyanobacterial Biology*. 18. Sci. Press, Beijing, pp. 128–132 (252–265).
- Hu, C.M., Lee, Z.P., Ma, R.H., Yu, K., Li, D.Q., Shang, S.L., 2010. Moderate resolution imaging spectroradiometer (MODIS) observations of cyanobacteria blooms in Taihu Lake, China. *J. Geophys. Res.-Oceans* (C4), 115.
- Hu, X.B., Zhang, R.F., Ye, J.Y., Wu, X., Zhang, Y.X., Wu, C.L., 2018. Monitoring and research of microcystins and environmental factors in a typical artificial freshwater aquaculture pond. *Environ. Sci. Pollut. R.* 25 (6), 5921–5933.
- Huang, W.J., Cheng, Y.L., Cheng, B.L., 2008. Ozonation by-products and determination of extracellular release in freshwater algae and cyanobacteria. *Environ. Eng. Sci.* 25 (2), 139–152.
- Huber, V., Wagner, C., Gerten, D., Adrian, R., 2012. To bloom or not to bloom: contrasting responses of cyanobacteria to recent heat waves explained by critical thresholds of abiotic drivers. *Oecologia* 169 (1), 245–256.
- Jiang, Y.G., Xiao, P., Liu, Y., Wang, J.X., Li, R.H., 2017. Targeted deep sequencing reveals high diversity and variable dominance of bloom-forming cyanobacteria in eutrophic lakes. *Harmful Algae* 64, 42–50.
- Joehnk, K.D., Huisman, J.E.F., Sharples, J., Sommeijer, B.E.N., Visser, P.M., Stroom, J.M., 2008. Summer heatwaves promote blooms of harmful cyanobacteria. *Glob. Chang. Biol.* 14 (3), 495–512.
- Joung, S.H., Oh, H.M., Ko, S.R., Ahn, C.Y., 2011. Correlations between environmental factors and toxic and non-toxic *Microcystis* dynamics during bloom in Daechung Reservoir, Korea. *Harmful Algae* 10 (2), 188–193.
- Kovacs, A.W., Toth, V.R., Vörös, L., 2012. Light-dependent germination and subsequent proliferation of N<sub>2</sub>-fixing cyanobacteria in a large shallow lake. *Ann. Limnol.-Int. J. Lim. EDP Sciences* 48 (2), 177–185.
- Kozak, A., Celewicz-Goldyn, S., Kuczyńska-Kippen, N., 2019. Cyanobacteria in small water bodies: the effect of habitat and catchment area conditions. *Sci. Total Environ.* 646, 1578–1587.
- Leão, P.N., Vasconcelos, M.T.S., Vasconcelos, V.M., 2009. Allelopathic activity of cyanobacteria on green microalgae at low cell densities. *Eur. J. Phycol.* 44 (3), 347–355.
- Leclerc, M., Saint-Hilaire, A., Bechara, J., 2003. State-of-the-art and perspectives of habitat modelling for determining conservation flows. *Can. Water Resour. J.* 28 (2), 135–151.
- Lehman, E.M., McDonald, K.E., Lehman, J.T., 2009. Whole lake selective withdrawal experiment to control harmful cyanobacteria in an urban impoundment. *Water Res.* 43 (5), 1187–1198.
- Lepš, J., Šmilauer, P., 2003. *Multivariate Analysis of Ecological Data Using CANOCO*. CUP.
- Li, Q.H., Chen, L.L., Chen, F.F., Gao, T.J., Li, X.F., Liu, S.P., et al., 2013. Maixi River estuary to the Baihua Reservoir in the Maotiao River catchment: phytoplankton community and environmental factors. *Chin. J. Oceanol. Limnol.* 31 (2), 290–299.
- Li, Y.P., Tang, C.Y., Yu, Z.B., Acharya, K.U.M.U.D., 2014. Correlations between algae and water quality: factors driving eutrophication in Lake Taihu, China. *Int. J. Environ. Sci. Technol.* 11 (1), 169–182.
- Li, X., Li, J.R., Li, C.Y., 2017. Ecological niche analysis of dominant phytoplankton species in Wuliangshui Lake, Inner Mongolia. *J. Hydroeco.* 38 (06), 40–47.
- Lins, R.P., Barbosa, L.G., Minillo, A., De Ceballos, B.S., 2016. Cyanobacteria in a eutrophicated reservoir in a semi-arid region in Brazil: dominance and microcystin events of blooms. *Braz. J. Bot.* 39 (2), 583–591.
- Liu, J.T., Fang, S.W., 2017. Comprehensive evaluation of the potential risk from cyanobacteria blooms in Poyang Lake based on nutrient zoning. *Environ. Earth Sci.* 76 (9), 342.
- Marshall, H.G., 2009. Phytoplankton of the York river. *J. Coast. Res.* 59–65.
- Martino, E.J., Able, K.W., 2003. Fish assemblages across the marine to low salinity transition zone of a temperate estuary. *Estuar. Coast. Shelf Sci.* 56 (5–6), 969–987.
- Maske, S.S., Sangolkar, L.N., Chakrabarti, T., 2010. Temporal variation in density and diversity of cyanobacteria and cyanotoxins in lakes at Nagpur (Maharashtra State), India. *Environ. Monit. Assess.* 169 (1–4), 299–308.
- Meng, R., He, L.S., Guo, L.G., Xi, B.D., Li, Z.Q., Shu, J.M., et al., 2013. Canonical correspondence analysis between phytoplankton community and environmental factors in macrophytic lakes of the middle and lower reaches of Yangtze River. *Huanjing Kexue* 34 (7), 2588–2596.
- Moller, C.L., Vangsøe, M.T., Sand-Jensen, K., 2014. Comparative growth and metabolism of gelatinous colonies of three cyanobacteria, *Nostoc commune*, *Nostoc pruniforme* and *Nostoc zetterstedtii*, at different temperatures. *Freshw. Biol.* 59 (10), 2183–2193.
- O'Boyle, S., McDermott, G., Silke, J., Cusack, C., 2016. Potential impact of an exceptional bloom of *Karenia mikimotoi* on dissolved oxygen levels in waters off western Ireland. *Harmful Algae* 53, 77–85.
- Palmer, M.W., 1993. Putting things in even better order: the advantages of canonical correspondence analysis. *Ecology* 74 (8), 2215–2230.
- Pang, C.C., Zhou, J., Zhang, X.J., Wu, S.Q., 2013. Experimental study on the influence of pH value, illumination, nutrient, and temperature factors on cyanobacteria growth. *IEEE* 747–750.
- Park, Y., Pyo, J., Kwon, Y.S., Cha, Y., Lee, H., Kang, T., et al., 2017. Evaluating physico-chemical influences on cyanobacterial blooms using hyperspectral images in inland water, Korea. *Water Res.* 126, 319–328.
- Park, B.S., Li, Z., Kang, Y.H., Shin, H.H., Joo, J.H., Han, M.S., 2018. Distinct bloom dynamics of toxic and non-toxic *Microcystis* (Cyanobacteria) subpopulations in Hoedong reservoir (Korea). *Microb. Ecol.* 75 (1), 163–173.
- Pettersson, K., Herlitz, E., Istvánovics, V., 1993. The role of *Gloeotrichia echinulata* in the transfer of phosphorus from sediments to water in Lake Erken. *Hydrobiologia* 253 (1–3), 123–129.
- Phlips, E.J., Badylak, S., Christman, M., Wolny, J., Brame, J., Garland, J., et al., 2011. Scales of temporal and spatial variability in the distribution of harmful algae species in the Indian River Lagoon, Florida, USA. *Harmful Algae* 10 (3), 277–290.
- Reynolds, C.S., Jaworski, G.H.M., Cmiech, H.A., Leedale, G.F., 1981. On the annual cycle of the blue-green alga *Microcystis aeruginosa* Kütz. emend. Elenkin. *Philos. Trans. R. Soc. Lond. B* 293 (1068), 419–477.
- Rigosi, A., Hanson, P., Hamilton, D.P., Hipsey, M., Rusak, J.A., Bois, J., Kim, B., 2015. Determining the probability of cyanobacterial blooms: the application of Bayesian networks in multiple lake systems. *Ecol. Appl.* 25 (1), 186–199.
- Scherer, P.L., Millard, A.D., Miller, A., Schoen, R., Raeder, U., Geist, J., et al., 2017. Temporal dynamics of the microbial community composition with a focus on toxic cyanobacteria and toxin presence during harmful algal blooms in two South German lakes. *Front. Microbiol.* 8, 2387.
- Sinden, A., Sinang, S.C., 2016. Cyanobacteria in aquaculture systems: linking the occurrence, abundance and toxicity with rising temperatures. *Int. J. Environ. Sci. Technol.* 13 (12), 2855–2862.
- Sivapragasam, C., Muttill, N., Muthukumar, S., Arun, V.M., 2010. Prediction of algal blooms using genetic programming. *Mar. Pollut. Bull.* 60 (10), 1849–1855.
- Soares, M.C.S., Rocha, M.I.D.A., Marinho, M.M., Azevedo, S.M., Branco, C.W., Huszar, V.L., 2009. Changes in species composition during annual cyanobacterial dominance in a tropical reservoir: physical factors, nutrients and grazing effects. *Aquat. Microb. Ecol.* 57 (2), 137–149.
- Spencer, D.F., Liow, P.S., Lembi, C.A., 2011. Growth response to temperature and light in *Nostoc spongiaforme* (Cyanobacteria). *J. Freshw. Ecol.* 26 (3), 357–363.
- Steffen, M.M., Davis, T.W., McKay, R.M.L., Bullerjahn, G.S., Krausfeldt, L.E., Stough, J.M., et al., 2017. Ecophysiological examination of the Lake Erie *Microcystis* bloom in 2014: linkages between biology and the water supply shutdown of Toledo, OH. *Environ. Sci. Technol.* 51 (12), 6745–6755.



- Su, M., Andersen, T., Burch, M., Jia, Z., An, W., Yu, J., Yang, M., 2019. Succession and interaction of surface and subsurface cyanobacterial blooms in oligotrophic/mesotrophic reservoirs: a case study in Miyun Reservoir. *Sci. Total Environ.* 649, 1553–1562.
- Tao, M., Duan, H.T., Cao, Z.G., Loisel, S.A., Ma, R.H., 2017. A hybrid EOF algorithm to improve MODIS cyanobacteria phycocyanin data quality in a highly turbid lake: bloom and nonbloom condition. *IEEE* 10 (10), 4430–4444.
- Teixeira de Oliveira, M., Rocha, O., Peret, A.C., 2011. Structure of the phytoplankton community in the Cachoeira Dourada reservoir (GO/MG), Brazil. *Braz. J. Biol.* 71 (3), 587–600.
- Tian, C., Pei, H.Y., Hu, W.R., Xie, J., 2013. Phytoplankton variation and its relationship with the environmental factors in Nansi Lake, China. *Environ. Monit. Assess.* 185 (1), 295–310.
- Tian, Y.Q., Huang, B.Q., Yu, C.C., Chen, N.W., Hong, H.S., 2014. Dynamics of phytoplankton communities in the Jiangdong Reservoir of Jiulong River, Fujian, South China. *Chin. J. Oceanol. Limnol.* 32 (2), 255–265.
- Tollefson, J., 2018. Forecasting efforts target harmful plankton blooms. *Nature* 555 (7698), 569–570.
- Vadas, R.L., Orth, D.J., 2001. Formulation of habitat suitability models for stream fish guilds: do the standard methods work. *T. Am. Fish. Soc.* 130 (2), 217–235.
- Vismara, R., Azzellino, A., Bosi, R., Crosa, G., Gentili, G., 2001. Habitat suitability curves for brown trout (*Salmo trutta fario* L.) in the River Adda, Northern Italy: comparing univariate and multivariate approaches. *Regul. River.* 17 (1), 37–50.
- Wang, X.Y., Yao, J.Y., Shi, Y., Su, T.L., Wang, L., Xu, J.P., 2016. Research on hybrid mechanism modeling of algal bloom formation in urban lakes and reservoirs. *Ecol. Model.* 332, 67–73.
- Werner, V.R., Laughinghouse IV, H.D., Fiore, M.F., Sant'Anna, C.L., Hoff, C., de Souza Santos, K.R., et al., 2012. Morphological and molecular studies of *Sphaerospermopsis torques-reginae* (Cyanobacteria, Nostocales) from South American water blooms. *Phycologia* 51 (2), 228–238.
- Wood, S.A., Atalah, J., Wagenhoff, A., Brown, L., Doehring, K., Young, R.G., et al., 2017. Effect of river flow, temperature, and water chemistry on proliferations of the benthic anatoxin-producing cyanobacterium *Phormidium*. *Freshw. Sci.* 36 (1), 63–76.
- Wu, Y.L., Li, L., Zheng, L.J., Dai, G.Y., Ma, H.Y., Shan, K., et al., 2016. Patterns of succession between bloom-forming cyanobacteria *Aphanizomenon flos-aquae* and *Microcystis* and related environmental factors in large, shallow Dianchi Lake, China. *Hydrobiologia* 765 (1), 1–13.
- Xiao, Y., Gan, N.Q., Liu, J., Zheng, L.L., Song, L.R., 2012. Heterogeneity of buoyancy in response to light between two buoyant types of cyanobacterium *Microcystis*. *Hydrobiologia* 679 (1), 297–311.
- Xu, H., Paerl, H.W., Qin, B.Q., Zhu, G.W., Gao, G., 2010. Nitrogen and phosphorus inputs control phytoplankton growth in eutrophic Lake Taihu, China. *Limnol. Oceanogr.* 55 (1), 420–432.
- Yang, H.J., Dai, R., Zhang, H.Y., Li, C.L., Zhang, X.Y., Shen, J.Z., et al., 2016. Production of monoclonal antibodies with broad specificity and development of an immunoassay for microcystins and nodularin in water. *Anal. Bioanal. Chem.* 408 (22), 6037–6044.
- Yang, J.W., Tang, H.X., Zhang, X.X., Zhu, X.X., Huang, Y., Yang, Z., 2018a. High temperature and pH favor *Microcystis aeruginosa* to outcompete *Scenedesmus obliquus*. *Environ. Sci. Pollut. R.* 25 (5), 4794–4802.
- Yang, K., Yu, Z.Y., Luo, Y., Yang, Y., Zhao, L., Zhou, X.L., 2018b. Spatial and temporal variations in the relationship between lake water surface temperatures and water quality—a case study of Dianchi Lake. *Sci. Total Environ.* 624, 859–871.
- Yuan, Y., Xiao, L.J., Han, B.P., 2015. Seasonal Dynamics of Cyanobacteria Assemblage in Tropical Large Reservoirs, South China—Using Dashahe and Gaozhou Reservoirs as Examples. *Ecol. Environ. Sci.* 24 (12), 2027–2034.
- Zhang, W., Zhang, X.L., Li, L., Zhang, Z.L., 2007. Urban forest in Jinan City: distribution, classification and ecological significance. *Catena* 69 (1), 44–50.
- Zhang, Z.G., Shao, Y.S., Xu, Z.X., 2010. Prediction of urban water demand on the basis of Engel's coefficient and Hoffmann index: case studies in Beijing and Jinan, China. *Water Sci. Technol.* 62 (2), 410–418.
- Zhang, Y.S., Li, H.Y., Yu, Y., Zhang, M., 2011. Role of colony intercellular space in the cyanobacteria bloom-forming. *Environ. Sci.* 32 (6), 1062–1067.
- Zhang, M., Zhang, Y.C., Yang, Z., Wei, L.J., Yang, W.B., Chen, C., et al., 2016. Spatial and seasonal shifts in bloom-forming cyanobacteria in Lake Chaohu: patterns and driving factors. *Phycol. Res.* 64 (1), 44–55.
- Zhao, L., Huang, W., 2014. Models for identifying significant environmental factors associated with cyanobacterial bloom occurrence and for predicting cyanobacterial blooms. *J. Great Lakes Res.* 40 (2), 265–273.
- Zhao, C.S., Liu, C.M., Xia, J., Zhang, Y.Y., Yu, Q., Eamus, D., 2012. Recognition of key regions for restoration of phytoplankton communities in the Huai River basin, China. *J. Hydrol.* 420, 292–300.
- Zhao, C.S., Sun, C.L., Liu, C.M., Xia, J., Yang, G., Liu, X.M., et al., 2014. Analysis of regional zoobenthos status in the Huai River Basin, China using two new ecological niche clustering approaches. *Ecohydrology.* 7, 91–101.
- Zhao, C.S., Yang, S.T., Xiang, H., Liu, C.M., Zhang, H.T., Yang, Z.L., et al., 2015a. Hydrologic and water-quality rehabilitation of environments for suitable fish habitat. *J. Hydrol.* 530, 799–814.
- Zhao, C.S., Yang, S.T., Liu, C.M., Dou, T.W., Yang, Z.L., Yang, Z.Y., et al., 2015b. Linking hydrologic, physical and chemical habitat environments for the potential assessment of fish community rehabilitation in a developing city. *J. Hydrol.* 523, 384–397.
- Zhao, C.S., Yang, S.T., Liu, J.G., Liu, C.M., Hao, F.H., Wang, Z.G., et al., 2018. Linking fish tolerance to water quality criteria for the assessment of environmental flows: a practical method for streamflow regulation and pollution control. *Water Res.* 141, 96–108.
- Zhu, R., Wang, H., Chen, J., Shen, H., Deng, X., 2018. Use the predictive models to explore the key factors affecting phytoplankton succession in Lake Erhai, China. *Environ. Sci. Pollut. R.* 25 (2), 1283–1293.
- Zi, J.M., Pan, X.F., MacIsaac, H.J., Yang, J.X., Xu, R.B., Chen, S.Y., et al., 2018. Cyanobacteria blooms induce embryonic heart failure in an endangered fish species. *Aquat. Toxicol.* 194, 78–85.